Transformation of ε-HBCD with the *Sphingobium Indicum* enzymes LinA1, LinA2 and LinATM, a triple mutant of LinA2

Norbert V. Heeb [a, *], Jasmin Hubeli [a, b, f], Thomas Fleischmann [c], Peter Lienemann [b], Namita Nayyar [d], Rup Lal [e], Hans-Peter E. Kohler [c]

[a] *Empa, Swiss Federal Laboratories for Materials Testing and Research, Laboratory for Advanced Analytical Technologies, Überlandstrasse 129, CH-8600, Dübendorf, Switzerland*
[b] *ZHAW, Zurich University of Applied Sciences, Institute of Chemistry and Biological Chemistry, Reidbach, CH-8820, Wädenswil, Switzerland*
[c] *Eawag, Swiss Federal Institute of Aquatic Science and Technology, Überlandstrasse 133, CH-8600, Dübendorf, Switzerland*
[d] *Sri Venkateswara College, University of Delhi, Delhi, 1110021, India*
[e] *The Energy and Resources Institute, India Habitat Center, New Delhi, Delhi, 110003, India*
[f] *Current Address: Cantonal Pharmacy Zürich, Südstrasse 3, CH-8952, Schlieren, Switzerland*

HIGHLIGHTS

- Implementation of the LinA1 substrate-binding site to LinA2 by point-directed mutagenesis.
- Expression of three LinA enzyme variants, LinA1, LinA2 and LinATM, in *E. coli* bacteria.
- Three of eight HBCD stereoisomers are converted by the dehydrohalogenase LinA2.
- All LinA variants follow Michaelis-Menten kinetics for the ε-HBCD transformation.
- Stereoselective conversion of ε-HBCD to 1E,5S,6R,9S,10R-PBCDen by LinA2.

GRAPHICAL ABSTRACT
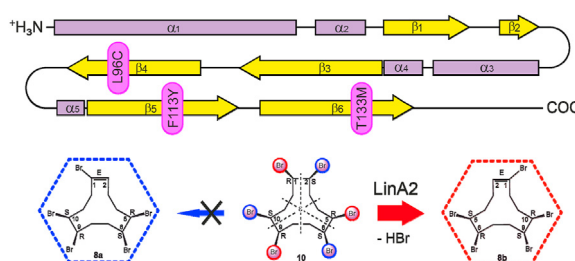
ARTICLE INFO

ABSTRACT

Hexabromocyclododecanes (HBCDs) were used as flame-retardants until their ban in 2013. Among the 16 stereoisomers known, ε-HBCD has the highest symmetry. This makes ε-HBCD an interesting substrate to study the selectivity of biotransformations. We expressed three LinA dehydrohalogenase enzymes in *E. coli* bacteria, two wild-type, originating from *Sphingobium indicum* B90A bacteria and LinATM, a triple mutant of LinA2, with mutations of L96C, F113Y and T133 M. These enzymes are involved in the hexachlorocyclohexane (HCH) metabolism, specifically of the insecticide γ-HCH (Lindane). We studied the reactivity of those eight HBCD stereoisomers found in technical HBCD. Furthermore, we compared kinetics and selectivity of these LinA variants with respect to ε-HBCD. LC-MS data indicate that all enzymes converted ε-HBCD to pentabromocyclododecenes (PBCDens). Transformations followed Michaelis-Menten kinetics. Rate constants k_{cat} and enzyme specificities k_{cat}/K_M indicate that ε-HBCD conversion was fastest and most specific with LinA2. Only one PBCDen stereoisomer was formed by LinA2, while LinA1 and LinATM produced mixtures of two PBCDE enantiomers at three times lower rates than LinA2. In analogy to the biotransformation of (−)β-HBCD, with selective conversion of dibromides in R-S-configuration, we assume that 1E,5S,6R,9S,10R-PBCDen is the ε-HBCD transformation product from LinA2. Implementing three amino acids of the LinA1 substrate-binding site into LinA2 resulted in a triple

* Corresponding author.
  E-mail address: norbert.heeb@empa.ch (N.V. Heeb).

mutant with similar kinetics and product specificity like LinA1. Thus, point-directed mutagenesis is an interesting tool to modify the substrate- and product-specificity of LinA enzymes and enlarge their scope to metabolize other halogenated persistent organic pollutants regulated under the Stockholm Convention.

1. Introduction

1.1. Polyhalogenated compounds and persistent organic pollutants

Radical-induced halogenation of various hydrocarbon precursors has been exploited in the past to produce polyhalogenated compounds at large scales. This approach can produce molecular libraries of hundreds of compounds differing in constitution and stereochemistry. For example, the non-specific chlorination of benzene leads to mixtures of nine hexachlorocyclohexane (HCH) stereoisomers. Only one of them, γ-HCH (Lindane) is the active insecticide, present at about 8–15% in technical HCH mixtures (Li, 1999; Vijgen et al., 2011). Pure γ-HCH was extracted from the crude product in later years while other HCHs remained as waste material (Vijgen et al., 2011). In 2009, α-, β- and γ-HCHs, the most abundant isomers in technical HCH mixtures, were included in the list of persistent organic pollutants (POPs) of the Stockholm Convention (SC) and HCH production and use were banned (UNEP, 2006; 2009).

The industrial production of dibromoethane, widely used as a scavenger in leaded gasolines, had to be reduced substantially when noble metal-based three-way catalysts were implemented in vehicles and non-leaded gasolines were introduced (Alaee et al., 2003). This brought about a remarkable shift in bromine use pattern and the advent of brominated flame-retardants (BFRs). Bromination of hydrocarbons is another example of a non-specific halogenation process that leads to mixtures of polybrominated materials. Bromination of 1,5,9-cyclododecatriene isomers yields mixtures consisting of at most 16 HBCD stereoisomers (Heeb et al., 2005). Fig. S1 (Supplementary material, SM) displays these stereoisomers. Constitutions of seven of the eight isomers found in technical HBCDs, have been deduced from crystal structure analysis (Heeb et al., 2005; 2007a; b, 2013).

HBCDs were high production volume chemicals too, produced at more than 10′000 t/y and used as flame-retardants, mainly in plastic and textile applications (Alaee et al., 2003). As HCHs are, also HBCDs are persistent, toxic, and accumulate along food chains (Tomy et al., 2004; Janak et al., 2005; Law et al., 2005; Kohler et al., 2008; Peck et al., 2008; Vorkamp et al., 2012). As certain isomers of such mixtures are transported over long distances, they reach even remote areas (de Wit et al., 2006). In 2013, after being used for about three decades, HBCDs were congruously added to the POP list of the Stockholm convention (UNEP 2013). Because these chemicals were produced and applied at large scales and are now ubiquitously distributed in the environment (de Wit, 2002; de Wit et al., 2006; Covaci et al., 2006; Marvin et al., 2011), they can be considered as markers of the anthropocene.

1.2. Evolution of POP-converting Sphingomonadacea bacteria

Several bacterial strains of the *Sphingomonadacea* family, that gained the ability to transform HCHs, have evolved in contaminated soils of HCH dumpsites in Japan, France and India (Imai et al., 1991; Nagasawa et al., 1993; Nagata et al., 1999, 2007; Trantirek et al., 2001; Kumari et al., 2002; Suar et al., 2005; Pal et al., 2005; Lal et al., 2006, 2010). In 2005, some of these *Sphingobium* strains were reclassified in three distinct species *S. indicum*, *S. japonicum*, and *S. francense* (Pal et al., 2005). These strains express several HCH-converting enzymes, among them the γ−HCH− (Lindane) converting dehydrohalogenase LinA, which was isolated in two forms named LinA1 and LinA2 (Nagasawa et al., 1993; Nagata et al., 1993, 1999; Pal et al., 2005). Both enzymes catalyze the elimination of hydrochloric acid from several HCHs (Suar et al., 2005; Bala et al., 2012).

Transformations of HCHs are stereoselective. LinA1 preferentially converts the (+)α−HCH−enantiomer, while LinA2 prefers the (−)α-HCH enantiomer (Suar et al., 2005). Product selectivity differs too and only specific pentachlorocyclohexene stereoisomers are formed (Suar et al., 2005; Shrivastava et al., 2017). Despite these differences, amino acid sequences of LinA1 and LinA2 are quite similar (90%), differing only by 15 out of 156 amino acids (Fig. 1.) Shrivastava et al. (2017) produced a series of single-, double- and triple-mutants of LinA enzymes by point-directed mutagenesis and identified those amino acids, involved in HCH recognition. The interactions of leucine L96, phenylalanine F113 and threonine T133 seem to be important for the positioning of both α-HCH enantiomers in the active site and with it affect the product selectivity of the enzyme (Fig. 1).

HCHs with diameters of 5–6 Å are relatively small compared to HBCDs (7–9 Å). Nevertheless, we hypothesized that HBCDs might also be suitable substrates for LinA enzymes and exposed 8 of the 16 HBCD stereoisomers (Fig. S1, SM) to LinA2. Evidence was found that both β-HBCD enantiomers are transformed by LinA2 (Heeb et al., 2014, 2015). The cleavage of C−Br bonds was found to be selective too and only few of the 32 possible pentabromocyclododecenes (PBCDens) were formed (Fig. S2, SM).

To get more insights into how LinA enzymes recognize and bind HBCD substrates, we expressed LinA1, LinA2 and LinATM, a triple mutant of LinA2, which includes three amino acids of the LinA1 substrate-binding site. We compared the reactivity and selectivity of these LinA variants and determined kinetic parameters and product selectivity of the transformations with ε-HBCD as the substrate. Despite the fact that the three LinA variants all contain the same catalytic dyad, their kinetics and selectivity varied substantially. This confirmed that substrate recognition is controlled by other amino acids that can be exchanged by point-directed mutagenesis. Such exchanges may lead to new LinA variants, with altered substrate and product specificity that may be used for biotransformation of other halogenated POPs.

2. Materials and methods

2.1. Materials, chemicals, buffers

Racemic mixtures of α-, β- and γ-HBCDs and the meso forms δ- and ε-HBCD were isolated from a technical HBCD mixture (Saytex HP-900 ®, mp = 168−184 °C) by normal phase liquid chromatography (LC) on silica with n-hexane/dichloromethane mixtures (Heeb et al., 2005). Diastereomerically pure materials were obtained for α-, β-, γ- and δ-HBCD by repetitive crystallization from
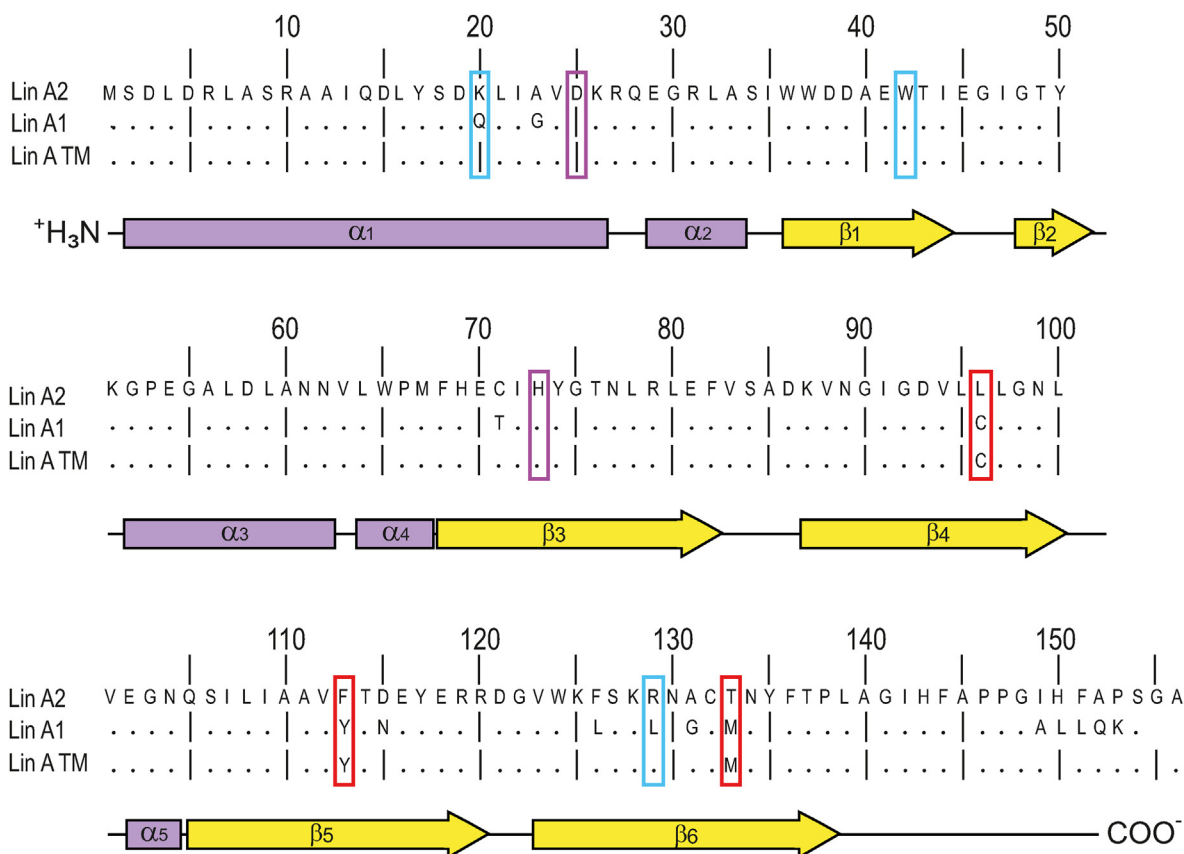
Fig. 1. Primary and secondary structures of three LinA variants. The one-letter amino acid nomenclature is used. LinA2 and the triple mutant LinATM consist of 156 amino acids with identical sequence except for three mutations L96C, F113Y and T133 M of the substrate-binding site (red), which were introduced by point-directed mutagenesis. The catalytic dyad (magenta) consists of D25 and H73. It is identical in all LinA variants. Two amino acids of the LinA2 halide-binding site (blue) differ from the one of LinA1, together with 13 other mutations. The secondary structure consists of five α−helices (violet) and six β-sheets (yellow). (For interpretation of the references to color in this figure legend, the reader is referred to the Web version of this article.)

dichloromethane/hexane mixtures. Respective crystal structure data has been reported (Heeb et al., 2005; 2007a; b, 2013). Acetonitrile (ROMIL, Cambridge, United Kingdom), dichloromethane (Merck, Darmstadt, Germany), n-hexane (Merck), methanol (Biosolve, Valkenswaard, Netherlands) and deionized water (Milli-Q, Merck) were used for LC. Glycine, imidazole, sodium phosphate, tris(hydroxethyl)amino methane (tris) (all from Sigma-Aldrich, Buchs, Switzerland) were used as buffer materials. Ampicillin, L-arabinose, chloramphenicol (Sigma-Aldrich), and lysogeny broth (AppliChem, Darmstadt, Germany) were used as growth media. Methoxy-pentabromocyclododecane (Empa, Switzerland) was used as internal standard.

2.2. Cloning, expression and purification of LinA enzymes

The expression of LinA1 and LinA2 has been described before (Geueke et al., 2013; Heeb et al., 2014). Codon-optimized *linA1* and *linA2* genes were obtained from John Oakeshott (CSIRO, Canberra, Australia). A modified *linA2* gene, which carried the desired mutations L96C, F113Y and T133 M, was also cloned. Briefly, codon-optimized (for expression in *E. coli*) *linA1/linA2* genes of *S. indicum* B90A and genes for the LinA triple mutant L96C, F113Y, T133M, synthesized by GeneArt (Germany), were cloned in a pDEST™17 vector. The plasmid pDEST17 was co-expressed in *E. coli* BL21-AITM cells with the pGro7 chaperone plasmid through heat shock transformation.

Three *E. coli* pre-cultures were produced. After addition of

inoculum (8 mL), three batches of cloned *E. coli* bacteria were fermented in lysogeny broth (800 mL), which contained ampicillin and chloramphenicol. Cells were grown over night at 37 °C to optical densities at 564 nm (OD_{564nm}) of 0.4−0.6. L-arabinose (1.6 g) was added and incubation was proceeded at 30 °C until OD_{564nm} of 1.8−2.0 were reached. Resulting cell material was harvested at 4 °C after centrifugation (10'000 rpm) and stored at −20 °C.

Disruption of cells by ultrasonification and isolation of the three LinA enzymes by affinity chromatography were performed following published procedures (Bala et al., 2012), which are described in detail in SM. Three solutions, with enzyme concentrations of 0.91, 2.06 and 0.50 mg mL^{-1}, were obtained for LinA1, LinA2 and LinATM, respectively, which were further used for exposure experiments.

2.3. Enzymatic incubation, workup, LC-MS-MS analyses

In five series of experiments racemic α-, β- and γ-HBCDs (8 μg) and δ- and ε-HBCDs (8 μg) were exposed to LinA2 for 2, 4, 8, 24 and 32 h in glycine-tris buffer (pH 8.3) with acetone (10%) as modifier. The role of acetone as a solubility enhancer for apolar compounds like HBCDs and CPs and its effect on the LinA2 enzyme have been tested and enzyme activity up to one week is documented (Heeb et al., 2014, 2019). In these experiments, we could observe conversion of substrates up to 32 h.

A second set of incubation experiments with ε-HBCD and LinA1, LinA2 and LinATM at five substrate/enzyme ratios $[S_o]/[E_o]$ of 10.8,

5.4, 2.7, 1.35 and 0.68 was performed. The enzyme concentration (0.58 μmol L^{-1}, m_{rel} = 17'342 Da), temperature and buffer conditions were identical in all exposure experiments. ε-HBCD was exposed for 0, 2, and 4 h to the three LinA variants at different [S$_o$]/[E$_o$] ratios and initial first-order rate constants k_{cat} were deduced. A detailed description of all incubation experiments is given in SM.

Separation of HBCDs and PBCDens was performed with a liquid chromatography (LC) system (Agilent 1290 Infinity, Santa Clara, CA, USA) with reverse phase- (RP) and chiral phase- (CP) columns. The RP-column (C$_{18}$-RP-SB, 50 mm × 3 mm, 1.8 μm, 100 Å, Agilent) was operated with a water-acetonitrile (A, 95/5 vol%) and methanol-acetonitrile-dichloromethane (B, 95/5/1 vol%) gradient (1 min 65% B, 65−90% B in 7 min, 1 min 90%, 90-65% B in 1 min, 2 min 65%) at a flow rate of 0.4 mL min^{-1}. The permethylated β-cyclodextrine CP-column (PM-β-CP, 200 mm × 4 mm, 5 μm, Nucleodex 5, Macherey-Nagel, Switzerland) was operated at a flow rate of 0.45 mL min^{-1} with a water (A) and methanol-dichloromethane (B, 100/0.5 vol%) gradient (65−82% B in 20 min, 85−98% B in 10 min, 2 min 98%, 98-65% in 2 min, 3 min 65%). Columns were kept at 50 °C.

Mass spectrometric analyses were performed on a triple-stage quadrupole MS (6460 TQ-MS, Agilent) with electrospray ionization in negative ion mode. Nebulizer- and sheath-gas temperatures of 325 and 340 °C with flow rates of 8 and 12 L min^{-1} and needle-, capillary-, fragmentor-, collision- and accelerator-voltages of 1500, 3000, 72, 7 and 6 V were applied. HBCDs and PBCDens were detected in multi-reaction monitoring mode (MRM), selecting the three most prominent chloride-adduct ions [M+Cl]$^-$ and recording transitions to bromide at m/z: 79 and 81. [M+Cl]$^-$ precursor ions at m/z: 674.7, 676.7, 678.7 were selected to detect HBCDs, precursor ions at 592.7, 594.7, 596.7 were monitored for PBCDens and ions at 626.7, 628.7, 630.7 were selected for methoxy-pentabromocyclododecane (IS).

2.4. Molecular docking experiments and graphical representations

Molecular docking experiments were performed with the AutoDock Vina software (Trott and Olson, 2010) as described before (Heeb et al., 2015). Input files in the pdbqt format were used for LinA2, the receptor, and for (+)β- and (−)β-HBCDs, the ligands, either in solid state or in activated conformations. Crystal structure data of LinA2 (Okai et al., 2010) was obtained from the protein database (PDB-ID: 3A76). Crystal structure data of β-HBCD enantiomers (Heeb et al., 2005, 2007a,b) can be obtained from CCDC (ID: 617557). Conformational adaptations were achieved with the Chem3D software. Graphical representations and geometrical parameters of enzyme-substrate complexes were obtained with PyMOL.

3. Results and discussion

3.1. Structural properties of LinA1, LinA2 and LinATM enzymes

The LinA2 crystal structure (Okai et al., 2010) is available from the protein database at a resolution of 2.24 Å (PDB-ID: 3A76). Fig. 1 displays the primary and secondary structures of the three LinA enzymes expressed in genetically modified *E. coli* bacteria. Highlighted are those amino acids (one letter code) involved in the catalytic center (magenta), the halide (blue) and the substrate binding sites (red). The catalytic dyad, consisting of aspartate (D25) and histidine (H73), is conserved in these enzymes. More variations are observed for the halide binding sites (Fig. 1, blue), which in case of LinA1 consists of glutamine (Q20), tryptophan (W42) and leucine (L129) and in case of LinA2 of lysine (K20), tryptophan (W42) and arginine (R129). The halide-binding site in LinATM is identical to

the one of LinA2, which is positively charged, while the one of LinA1 is not. The secondary structure consists of five α−helices (violet) and six β-sheets (yellow) (Fig. 1).

From previous work on α-HCHs and several single-, double- and triple-mutants of LinA (Shrivastatava et al., 2017) and own considerations, we hypothesized that the amino acids leucine (L96), phenylalanine (F113) and threonine (T133) may also be involved in substrate recognition and binding of HBCDs (Fig. 1, red). By point-directed mutagenesis, we produced a triple mutant of LinA2, replacing leucine by cysteine (L96C), phenylalanine by tyrosine (F113Y) and threonine by methionine (T133M). These amino acids are located in the antiparallel β-sheet structure (β4, β5, β6) in the inner surface of the cone-like protein (Fig. 1). These mutations are expected to alter the substrate binding specificity, which is different for LinA1 and LinA2. LinA1 preferentially binds (+)α-HCH, while LinA2 prefers (−)α-HCH (Suar et al., 2005).

Fig. 2 displays views of the tertiary and quaternary structures (ribbon form) of LinA2. The tertiary structure of LinA2 is expected to also represent those of LinA1 and LinATM. The structure consists of an extended antiparallel β-sheet, which forms a narrow cone (Fig. 2A). A long α-helix (Fig. 1, α$_1$) supports the cone structure. A shorter second helix is located at the entrance of the cone, the later has an inner diameter of about 8−11 Å. The catalytic dyad, the halide- and the substrate-binding sites are all located within the cone. In other words, substrates must access the inner space of the cone and products must be released from it to allow a productive catalytic cycle. Fig. 2B and C displays the quaternary structure of a LinA2 homo-trimer. The three cones arrange in a trifold symmetry (C$_{3v}$) with the extended beta-sheets in close contact, while the long α$_1$-helices all point in the same direction, forming the tip of the triple cone. Fig. 2D highlights apolar amino acid residues in yellow, indicating that hydrophobic interactions are stabilizing the quaternary structure of the LinA2 trimer.

3.2. Stereoselective transformation of HBCDs with LinA2

Sphingobium bacteria expressing LinA enzymes have evolved in HCH-contaminated soils at geographically distinct locations (Pal et al., 2005). HCH and their pentachlorocyclohexene transformation products have diameters of 5−6 Å. We hypothesized that some of the 16 HBCD stereoisomers (Fig. S1, SM), with diameters of 7−9 Å, might also be suitable LinA substrates, binding the active site in productive ways.

We exposed racemic mixtures of α-, β- and γ-HBCDs and the meso forms δ- and ε-HBCDs to LinA2 and could detect by LC-MS a substantial conversion of β- and ε-HBCDs and the appearance of two major and one minor PBCDen product. Fig. S3 compares MRM mass traces of chloride adducts [M+Cl]$^-$ of HBCDs and PBCDens. The precursor ions at m/z: 674.7, 676.7 and 678.6 (left) and m/z: 592.7, 594.7 and 596.7 (right) were monitored during fragmentation to bromide ions at m/z: 79 and 81 before (t = 0 h) and after LinA2 exposure (t = 32 h). On a column with a chiral β-cyclodextrin phase, we could separate α- (A), β- (B) and γ-HBCD (C) enantiomers into two peaks, while the meso forms δ- (D) and ε-HBCD (E) only formed single peaks. Optical activities of different enantiomers have been assigned before (Heeb et al., 2005). Fig. S4 displays LC-MS results from a C18-reverse phase column, on which HBCD diastereomers but not enantiomers can be resolved.

Fig. S3 also indicates that substantial amounts of (−)β-HBCD (B) and ε-HBCD (E) are converted by LinA2. Accordingly, two PBCDen products (highlighted) were formed, eluting after 25.8 and 27.3 min from the β-cyclodextrin column. In addition, smaller amounts of (+)β-HBCD were transformed to a PBCDen eluting after 29.1 min. Fig. S2 displays all 16 E-PBCDen configurations possible. Accordingly, 16 Z-PBCDens may be expected. Chromatographic retention
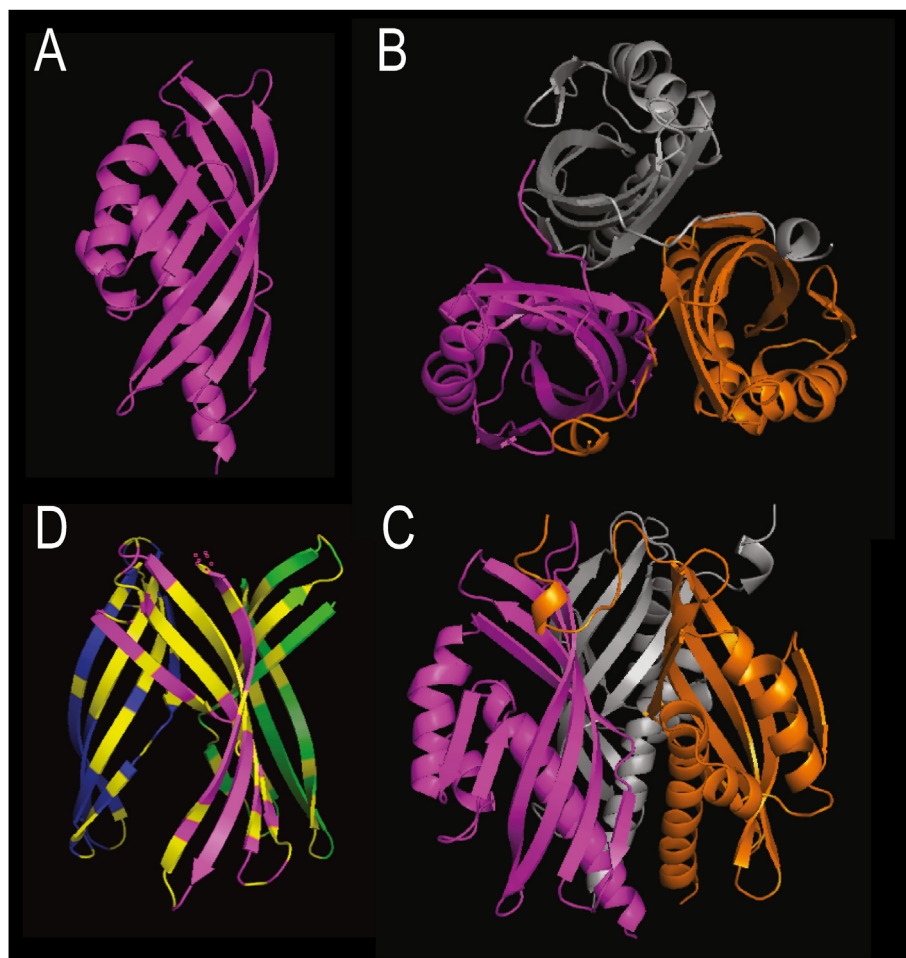
Fig. 2. Tertiary (A) and quaternary structures (B, C) of LinA2, which forms a homotrimer. The crystal structure was obtained from the protein database (PDB-ID: 3A76). The three monomers colored in magenta, orange and gray are oriented in C_3-symmetry. Amino-termini are in close vicinity and equally oriented. The cone-like structure can be seen from top (B) and from the side (C). The catalytic dyad, the halide- and the substrate-binding sites are located inside the cone. Highlighted in yellow (D) are lipophilic amino acids which cluster in the β_4-and β_5-strands. They are responsible for hydrophobic contacts and the assembly of the trimer. (For interpretation of the references to color in this figure legend, the reader is referred to the Web version of this article.)

times of HBCDs and PBCDens on RP- and CP-columns are given in Table S1 (SM). We conclude that three of eight exposed HBCD stereoisomers fit into the active site of LinA2 and were converted to only three PBCDen stereoisomers. Thus, LinA2 was both, substrate- and product-selective.

In Fig. 3A and B, we delineate the stereochemical preferences of LinA1 and LinA2, which convert $(+)\alpha$- and $(-)\alpha$-HCH to the respective pentachlorocyclohexenes. In Fig. 3C, the LinA2-catalyzed transformation of $(-)\beta$-HBCD to 1E,5R,6R,9S,10R-PBCDen (3a) but not to its 1E,5S,6S,9R,10S-enantiomer (3b) is delineated. Fig. 3D displays the symmetrical ε-HBCD configuration with three mirror planes (dashed lines) and a C_{3v}-symmetry. Due to the three-fold symmetry axis, stereocenters at C1, C5 and C9 in R-configuration and those at C2, C6 and C10 in S-configuration are superimposable. As a consequence, only two HBr elimination products with the 1E,5R,6S,9R,10S (8a) and the 1E,5S,6R,9S,10R (8b) configuration can be expected. These PBCDens are enantiomers and, in principle, can be separated on a chiral-phase column (Fig. S3) but not on a RP column (Fig. S4). Chromatographic evidence indicates that only one PBCDen product was formed during the LinA2-catalyzed transformation of ε-HBCD (Fig. S3), while two products were obtained after LinA1 exposure (Fig. 4). Thus, the ε-HBCD transformation with LinA2 is stereo- and regio-selective too, like the ones of $(-)\alpha$-HCH

(Suar et al., 2005) and $(-)\beta$-HBCD (Heeb et al., 2015).

3.3. Stereoselectivity of the ε-HBCD transformation with three LinA variants

We used ε-HBCD to probe the stereoselectivity of the dehydrohalogenases LinA1, LinA2 and a triple-mutant LinATM with mutations L96C, F113Y and T133M. Other LinA variants, like those single-, double- and triple-mutants tested for α-HCHs by Shrivastava et al. (2017), might be interesting candidates too to identify those amino acids affecting the transformation of HBCDs.

Herein, we compared the kinetics and selectivity of these three LinA variants and exposed them to ε-HBCD at five different substrate/enzyme ratios $[S_o]/[E_o]$. Fig. 4 displays chromatographic evidence (CP) that all LinA variants converted some ε-HBCD to PBCDens. LinA2 converted nearly all of the given ε-HBCD in 32 h (Fig. 4A), while substantial amounts of substrate remained in case of LinA1 and LinATM (Fig. 4B and C). Accordingly, large amounts of a single PBCDen product were formed by LinA2, while only small amounts of two PBCDen products were observed after LinA1 and LinATM exposure. These findings are confirmed from RP-LC-MS data (Fig. S5, SM) with the difference that both PBCDen enantiomers 8a and 8b appear as one single peak on the RP column.
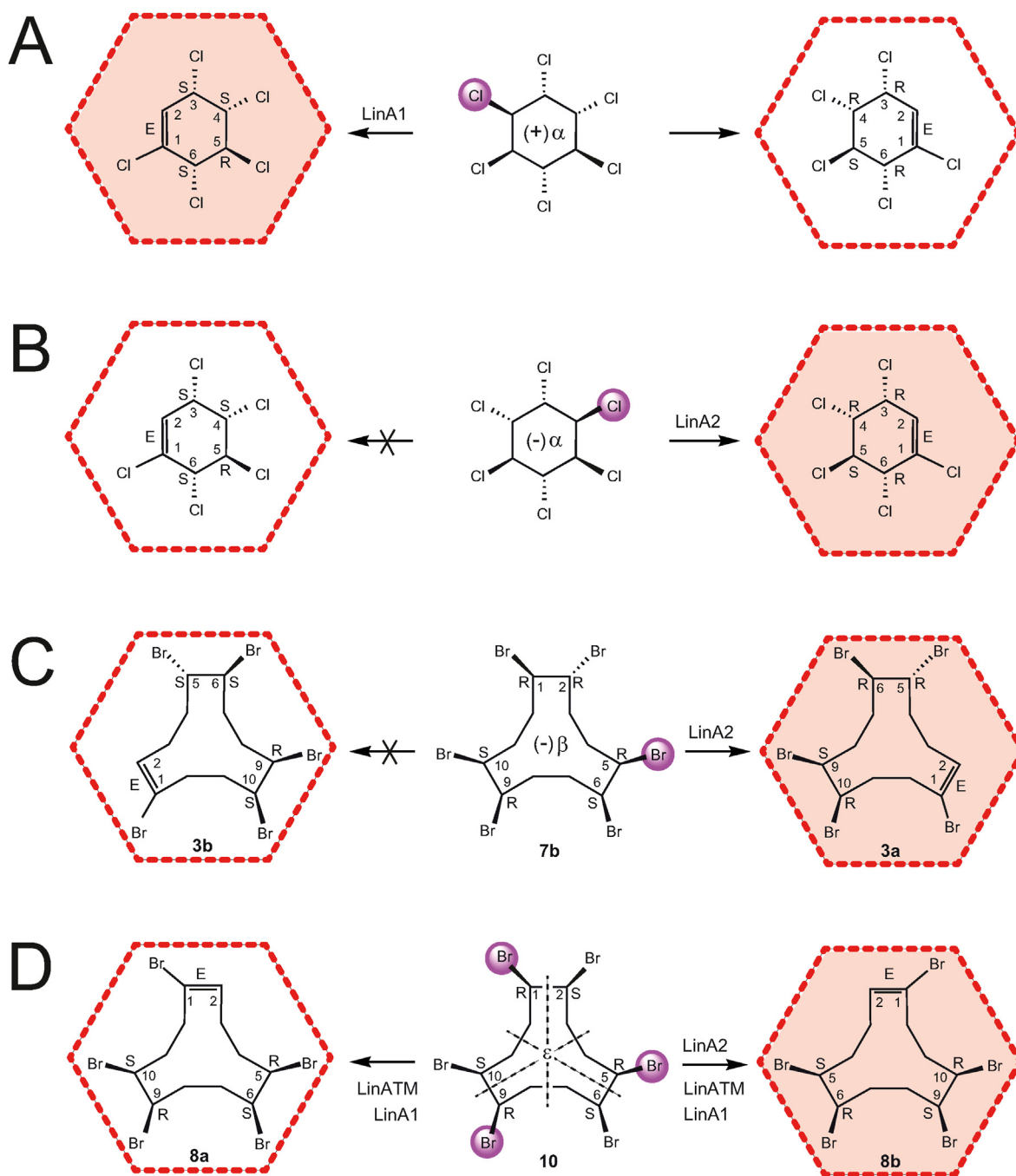
Fig. 3. Regio- and stereoselective dehydrohalogenations of $(+)\alpha$-HCH (A) by LinA1 and of $(-)\alpha$-HCH (B), $(-)\beta$-HBCD (C) and ε-HBCD (D) by LinA2. The dehydrobromination of highly symmetrical ε-HBCD (D), with three mirror planes (dashed lines) and a C_3-rotation axis, can lead to only two PBCDens. Elimination of bromines at C1, C5 and C9, which all are in R-configuration, lead to PBCDen 8b (D, right). Accordingly, bromine losses at C2, C6 and C10, which are in S-configuration, lead to the PBCDen enantiomer 8a (D, left). The LinA2-catalyzed transformation of $(-)\beta$-HBCD (7b) to 1E,5R,6R,9S,10R-PBCDen 3a (C) and the one of $(-)\alpha$-HCH to 1E,3R,4R,5S,6R-pentachlorocyclohexene (B) are stereoselective too. The $(+)$-α-HCH enantiomer is preferentially transformed by LinA1 (A), but not by LinA2. Assigned HBCD and PBCDen structures refer to the numbering in Figures S1 and S2 (SM). Leaving halides are highlighted in magenta.

Small amounts of two PBCDen isomers can be detected in the starting material as well (Fig. 4, t = 0 h). They eluted after 26.7 and 27.2 min from the CP column and were assigned to PBCDen 8a and 8b too.

3.4. Michaelis-Menten kinetics of ε-HBCD transformations with three LinA variants
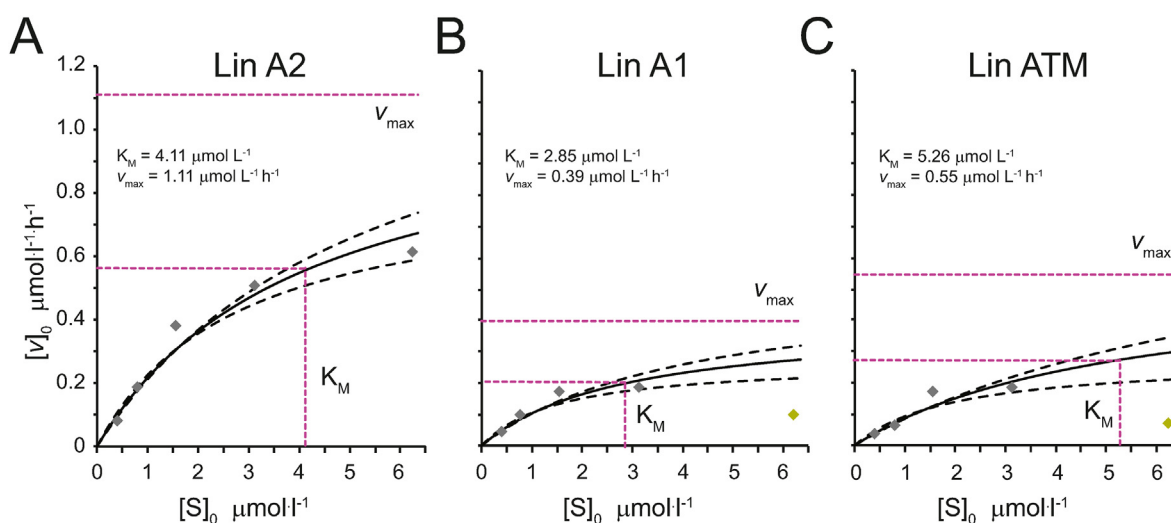
Initial rates (v_o) for the transformation of ε-HBCD by LinA1,

LinA2 and LinATM were determined for five $[S]_o/[E]_o$ ratios which varied from 10.8 to 5.4, 2.7, 1.35 and 0.68 at enzyme concentrations of 10 mg L^{-1} (0.58 μmol L^{-1}, m_{rel} 17.3 kDa).

Initial rates were deduced from linear regression models shown in Fig. S6 (SM). As shown in Fig. 5, hyperbolic dependences are obtained when plotting initial rates v_o (μmol L^{-1} h^{-1}) versus initial substrate concentrations $[S]_o$ (μmol L^{-1}), as expected for Michaelis-Menten kinetics. Observed (symbols) and modeled (lines) data of the ε-HBCD conversion with LinA2, LinA1 and LinATM are
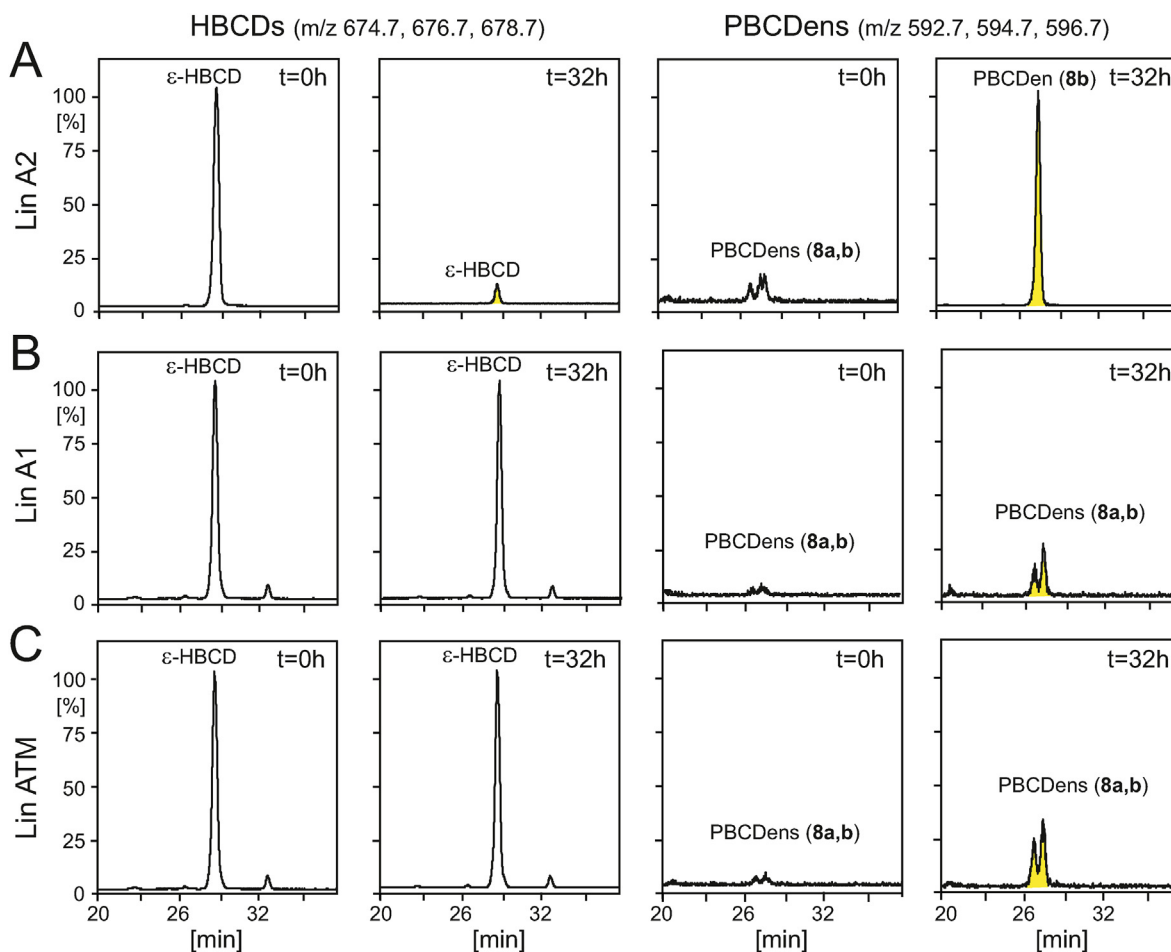
Fig. 4. Chiral-phase (CP) chromatograms of ε-HBCD and its PBCDen transformation products before and after exposure with LinA2 (A), LinA1 (B) and LinATM (C). Multiple reaction monitoring (MRM) was applied, observing three intense chloride-adduct ions [M+Cl]⁻ of HBCDs (*m/z*: 674.7, 676.7, 678.7) and PBCDens (*m/z*: 592.7, 594.7, 596.7) and their fragmentation to bromide (*m/z*: 79, 81). A permethylated β-cyclodextrin column was used. The meso-form ε-HBCD (left) elutes as a single peak from the CP-column. Significant amounts of ε-HBCD were transformed by LinA2 to PBCDen 8b (A, right). Traces of both PBCDen enantiomers 8a and 8b are found in the starting material. Nevertheless, PBCDens 8a and 8b were also formed during LinA1 (B) and LinATM (C) exposure. Assigned PBCDen structures refer to the numbering in Figure S2 (SM).

Fig. 5. Michaelis-Menten kinetics of the ε-HBCD conversion with three LinA variants. First-order initial rate constants v_0 for the transformation of ε-HBCD with the LinA variants were determined from short exposure experiments (0, 2, 4 h) with different substrate/enzyme ratios $[S]_o/[E]_o$ of 10.8, 5.4, 2.7, 1.35 and 0.68. From these data, hyperbolic regression models were deduced for LinA2 (A), LinA1 (B) and LinATM (C). Respective fits of the dependence of reaction rates and substrate concentrations lead to Michaelis-Menten parameters K_M and v_{max}, which are indicated and listed in Table S2 (SM).

compared. Conversion of ε-HBCD was fastest with LinA2.

Table S2 (SM) lists Michaelis-Menten parameters, deduced from these hyperbolic regression models (Fig. 5). Maximal reaction rates (v_{max}) of 1.11 ± 0.09, 0.39 ± 0.04 and 0.55 ± 0.09 μmol L^{-1} h^{-1} were not reached in the observed concentration range. Michaelis-Menten constants K_M of LinA2, LinA1 and LinATM were 4.1 ± 0.5, 2.9 ± 0.4 and 5.3 ± 1.1 μmol L^{-1}, respectively (Table S2). Thus, K_M of LinA2 and LinATM were similar, the one of LinA1 was about two times lower, indicating that LinA1 binds ε-HBCD tighter. Respective first-order rate constants k_{cat} were 1.92 ± 0.16, 0.68 ± 0.07 and 0.95 ± 0.16 h^{-1}. Thus, ε-HBCD was converted three times faster by LinA2 than by LinA1, and conversion by the LinATM was half as fast as the one of LinA2.

Respective enzyme specificities k_{cat}/K_M decreased from 130 ± 25 to 66 ± 17 and 50 ± 19 L mol^{-1} s^{-1} for LinA2, LinA1 and LinATM, respectively. In other words, LinA2 had the highest specificity (Fig. 5).

Table S2 also includes v_{max}, K_M and k_{cat}/K_M of the (−)β-HBCD conversion by LinA2, which were 0.17 ± 0.01 μmol L^{-1} h^{-1}, 0.47 ± 0.07 μmol L^{-1} and 178 ± 36 L mol^{-1} s^{-1}, respectively (Heeb et al., 2014). Thus, v_{max} of the (−)β-HBCD conversion was about seven times slower than the one of ε-HBCD. Because K_M was nine times lower, the overall enzyme specificity k_{cat}/K_M for (−)β-HBCD was slightly higher than the one for ε-HBCD.

We conclude that the three point mutations introduced in the substrate-binding site lowered the rate and product selectivity of LinATM to values observed for LinA1. In other words, LinA2 has the highest rate and product selectivity for ε-HBCD, while the triple mutant with lower selectivity, might preferentially bind larger substrates.

3.5. Regio- and stereoselective transformation of ε-HBCD by LinA2

Configurations of ε-HBCD (10) and both β-HBCD enantiomers (7a/b) are very similar (Fig. S1, SM). They differ only in one chiral center as indicated in Fig. 6 (blue circles). Inversion at C2 of (+)β-HBCD (Fig. 6A) from S- to R-configuration results in ε-HBCD in the conformation given in Fig. 6C. Accordingly, an inversion at C2 of (−)β-HBCD (Fig. 6B) from R to S-configuration results in ε-HBCD in the enantiomeric conformation (Fig. 6D). Both ε-HBCD conformations shown in Fig. 6C and D are enantiomeric (dashed lines) and in equilibrium. In other words, both conformations are energetically equal and found in a 1/1 mixture. Thus, ε- and β-HBCDs have related configurations and conformations and may interacted likewise with LinA enzymes.

In analogy, we assume that both ε-HBCD conformations (Fig. 6C and D) can bind to LinA2 like both β-HBCDs (Fig. 6A and B). Thus, the enzyme catalyzes the cleavage of those bromine atoms highlighted in magenta (Fig. 6). Interestingly, both pathways starting with the ε-HBCD conformations shown in Fig. 6C and D lead to the same PBCDen product 8b with the 1E,5S,6R,9S,10R configuration (Fig. 6E). Thus, only one product is expected *in silico* for the LinA2-catalyzed transformation of ε-HBCD, which is in accordance with experimental data (Fig. 4).

Fig. 7A,B displays the activated (*) conformations of (+)β- and (−)β-HBCD as they bind to LinA2 according to docking experiments (Heeb et al., 2015). These substrate-enzyme complexes seem reasonable. In case of the (−)β-HBCD-complex, the predicted PBCDen product 3a (Fig. S2) was in accordance with the observed product. The findings confirm that LinA2-catalyzed transformations of both β-HBCD enantiomers are regio- and stereoselective. Only those bromine atoms highlighted at positions C10 in

(+)β-HBCD (Fig. 6A) and at C5 in (−)β-HBCD (Fig. 6B), are recognized by the halide binding site. Both carbon atoms are in R-configurations and part of vicinal dibromides with left-handed synclinal orientations (-sc).

In analogy, we postulate that both ε-HBCD conformations (Fig. 6C and D) also bind to LinA2 like (+)β- and (−)β-HBCD. Respective enzyme-substrate complexes are displayed in Fig. 7C and D. Those bromides released by LinA2 bind to the halide-binding site (Fig. 7, red). As mentioned, both enzyme-substrate complexes (Fig. 7C and D) lead to the same PBCDen product 8b with the 1E,5S,6R,9S,10R-configuration (Fig. 6E). Those bromine atoms of ε-HBCD differing from the ones of β-HBCDs are highlighted in magenta (Fig. 7C and D). They are not in vicinity to the catalytic dyad and the halide-binding site and are not directly involved in the catalytic cycle but may have a role in substrate recognition.

4. Conclusions

The large-scale application of HCHs as insecticides, until the ban in 2009, has led to a global contamination and a chronic exposure of biota to low levels of these compounds. Prolonged exposure of certain *Sphingobium* bacteria to high HCH concentrations directed bacterial evolution and resulted in the appearance of new dehydrohalogenases like LinA1 and LinA2. LinA1 and LinA2 sequences are highly conserved, but substrate recognition differs. Shrivastava et al. (2017) studied the substrate specificity of several LinA mutants, among them single-, double- and triple-mutants, with respect to α-HCHs. Based on this study and our own work, we postulated that amino acids L96, F113 and T133 of LinA2 might affect substrate orientation of HBCDs too. With three point mutations (L96C, F113Y, T133M), we imbedded the substrate binding site of LinA1 into LinA2. These three mutations altered the kinetics (k_{cat}), the catalytic specificity (k_{cat}/K_M) and the product selectivity.

The release of HBr from (−)β-, (+)β- and ε-HBCD by LinA2 is both, regio- and stereo-selective leading to only one PBCDen product for each HBCD stereoisomer but not to the respective enantiomers. So far, (−)β-, (+)β- and ε-HBCDs are the only brominated substrates known that are converted by LinA enzymes. Lately, we showed that also certain chlorinated paraffins are substrates for LinA2 (Heeb et al., 2019).

As shown, we could alter the substrate- and product-specificity of LinA enzymes with three point mutations. The exchange of leucine to cysteine (L96C) induced a volume reduction of −52 Å^3 in the substrate-binding site. Slightly more steric strain is introduced by F113Y ($+6$ Å^3) and T133 M ($+31$ Å^3) mutations. Overall, more space is offered in the substrate binding site of the LinATM, which lowered both, the rate and selectivity of the dehydrohalogenation reaction. Other properties such as the polarity, the hydrogen-bonding properties or the electronic structure might have changed too by these mutations. Specific mutations of these three positions seem promising for future studies and may help to design new dehydrohalogenases to convert other persistent organic pollutants. Thus, more extensive exploration of the role of amino acids near the active site is a prerequisite to further engineer LinA enzymes with changed substrate specificities. Well-designed dehydrohalogenases might be useful in bioremediation of contaminated sites (Lal et al., 2010).

Bacterial transformation of HBCDs may play a role in the environment too. The absence of certain HBCD stereoisomers such as β-, δ- and ε-HBCDs in environmental samples, and the accumulation of others, such as α- and γ-HBCDs (Tomy et al., 2004; Janak et al., 2005; Zegers et al., 2005; Kohler et al., 2008; Peck et al., 2008;
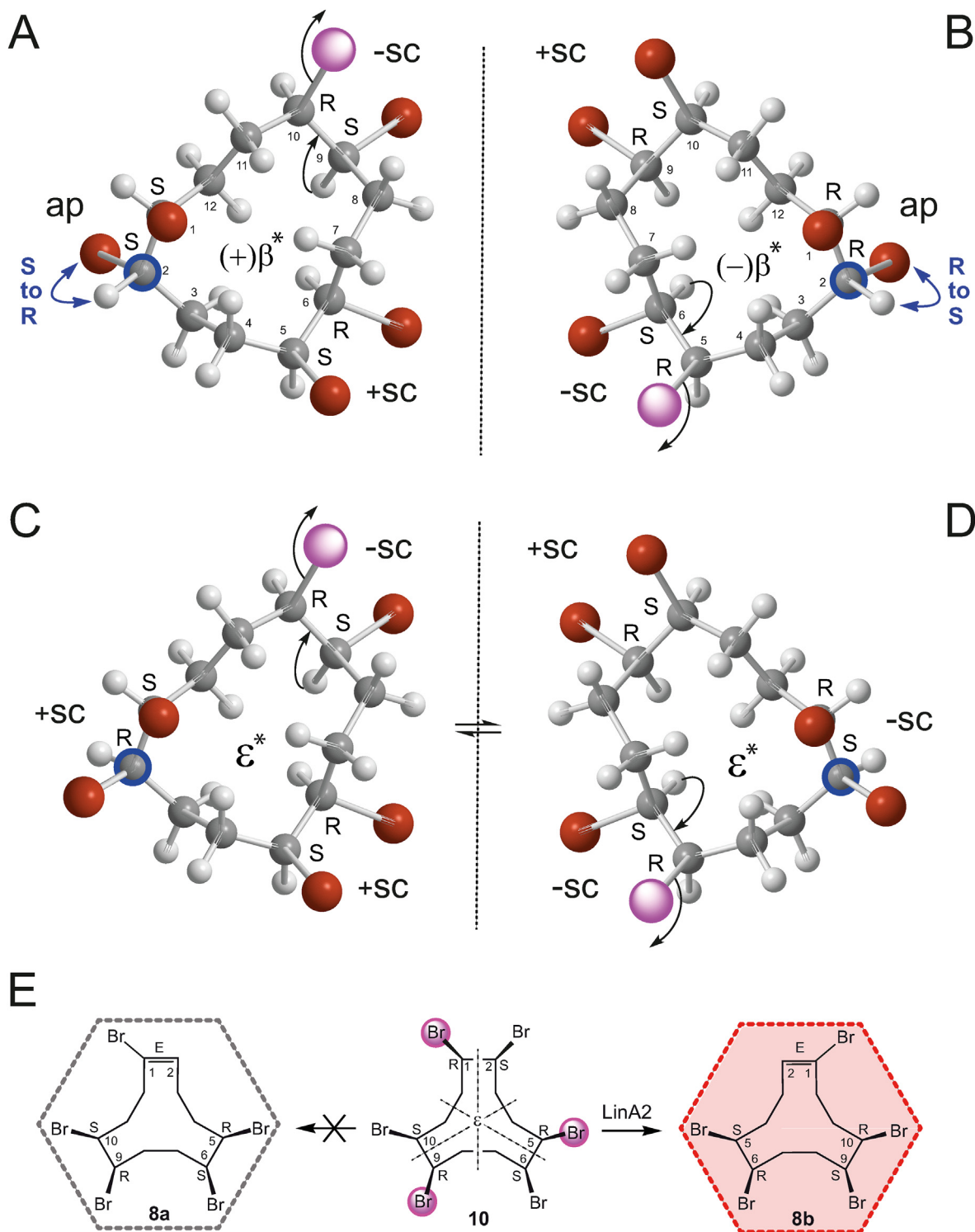
Fig. 6. Postulated reactive conformations of β- and ε-HBCDs. Two activated (*) conformations of (+)β-HBCD (A) and (−)β-HBCD (B) were found to bind to LinA2 *in silico* docking experiments (Heeb et al., 2015). Binding to LinA2 in activated form (induced fit), catalyzes the regio- and stereoselective loss of bromides (magenta) from C10 (A) and C5 (B). Configurations of β- and ε-HBCDs are identical for 5 out of 6 stereocenters. Inversion of configurations at C2 (blue) of (+) and (−)β-HBCDs from S to R and from R to S, respectively, results in those two ε-HBCD conformations shown in C and D. Assuming that these ε-HBCD conformations bind to LinA2 as well, only one transformation product is expected. PBCDen 8b (E) with the 1E,5S,6R,9S,10R configuration, but not its enantiomer PBCDen 8a (E) is the expected product. (For interpretation of the references to color in this figure legend, the reader is referred to the Web version of this article.)
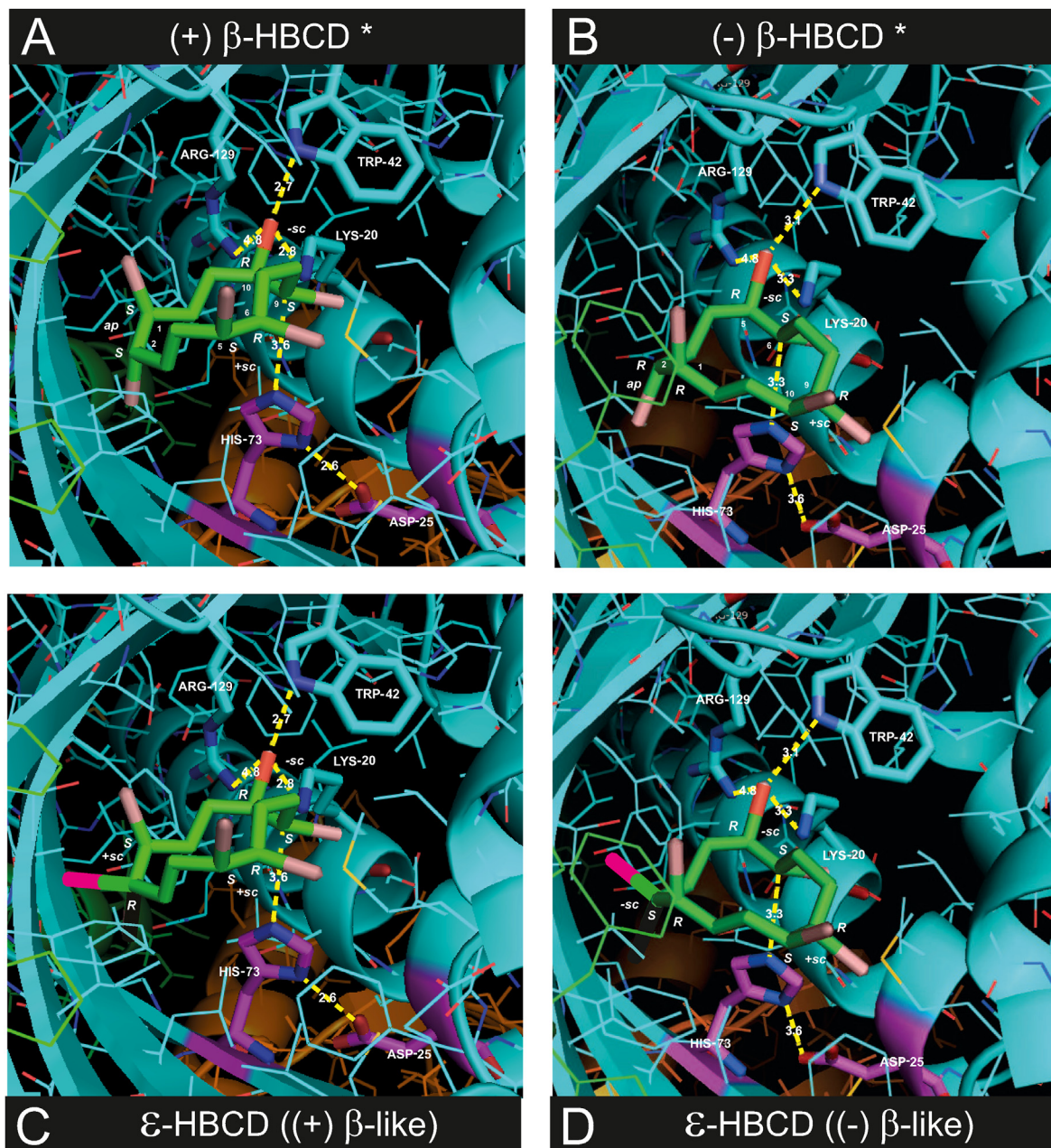
Fig. 7. Views of enzyme-substrate complexes of LinA2 with (+)β-HBCD (A), (−)β-HBCD (B) and two ε-HBCD conformations (C, D). Views through the 8−11 Å wide cleft into the cone are shown. Docking experiments resulted in two productive enzyme-substrate complexes with two activated (*) β-HBCD conformations. One dibromide with antiperiplaner (ap) and two with synclinal (sc) orientations are present in (+)β- (A) and (−)β-HBCD (B). Inversion at C2 of (+)β-HBCD (A) from S to R produces ε-HBCD in the conformation C, with two dibromides in +sc and one in −sc orientation. Accordingly, inversion at C2 of (−)β-HBCD (B) from R to S produces ε-HBCD in conformation D, with two dibromides in −sc and one in +sc orientation. In each case (A−D), dibromides in −sc orientations are bound to the active site (magenta) and leaving bromides in R-configurations are in close contact to the positively charged halide-binding site. The leaving bromides are coordinated by three nitrogen atoms in distances of 2.7−4.8 Å (dashed lines) of K20, W42 and R129. The catalytic dyad of D25 and H73 (magenta) acts as a base, binding hydrogen atoms from the backside, in α-positions to the leaving bromides. These four enzyme-substrate complexes (A−D) are similar with respect to active site geometry. They allow 1,2-diaxial eliminations of HBr leading to PBCDens 5b and 3a, when starting with (+)β- and (−)β-HBCD (A,B). PBCDen 8b is the expected product for both ε-HBCD-enzyme complexes (C,D).

Vorkamp et al., 2012) may be explained by selective enzymatic transformations. This has been observed *in-vitro* for LinA and LinB (Heeb et al., 2013, 2015, 2018).

In conclusion, despite the proven persistence of polyhalogenated pollutants at least some of these compounds can be dehalogenated by certain enzymes, expressed in bacteria of the *Sphingobium* family. By directed or random biological evolution, these enzymes may be further optimized to convert other POPs, regulated under the Stockholm Convention.

Credit author statement

Research ideas and design of the LinA mutant were developed by N.V.H., P.L., R.L. and H.-P.E.K. Cloning of LinA genes and their transfer into plasmid vectors and into E.coli was performed by T.F, N.N. and H.-P.E.K. Cell cultivation, expression and purification of the three LinA variants was acchieved by J.H. and T.F. Exposure experiments, mass spectrometric and chromatographic characterization and data analyses were performed by J.H. and N.V.H. The

manuscript was written by J.H. and N.V.H. All authors have discussed the results, reviewed and approved the manuscript.

Declaration of competing interest

Acknowledgements

Appendix A. Supplementary data

Supplementary data to this article can be found online at https://doi.org/10.1016/j.chemosphere.2020.129217.

References

Alaee, M., Arias, P., Sjödin, A., Bergman, A., 2003. An overview of commercially used brominated flame retardants, their applications, their use patterns in different countries/regions and possible modes of release. Environ. Int. 29, 683–689.

Bala, K., Geueke, B., Miska, M., Rentsch, D., Poiger, T., Dadhwal, M., Lal, R., Holliger, C., Kohler, H.-P.E., 2012. Enzymatic conversion of ε-hexachlorocyclohexane and a heptachlorocyclohexane isomer, two neglected components of technical hexachlorocyclohexane. Environ. Sci. Technol. 46, 4051–4058.

Covaci, A., Gerecke, A.C., Law, R.J., Voorspoels, S., Kohler, M., Heeb, N.V., Leslie, H., Allchin, C.R., De Boer, J., 2006. Hexabromocyclododecanes (HBCDs) in the environment and humans: a review. Environ. Sci. Technol. 40, 3679–3688.

de Wit, C.A., 2002. An overview of brominated flame retardants in the environment. Chemosphere 46, 583–624.

de Wit, C.A., Alaee, M., Muir, D.C.C., 2006. Levels and trends of brominated flame retardants in the Arctic. Chemosphere 64, 209–233.

Geueke, B., Garg, N., Ghosh, S., Fleischmann, T., Holliger, C., Lal, R., Kohler, H.-P.E., 2013. Metabolomics of hexachlorocyclohexane (HCH) transformation: ratio of LinA to LinB determines metabolic fate of HCH isomers. Environ. Microbiol. 15, 1040–1049.

Heeb, N.V., Schweizer, W.B., Kohler, M., Gerecke, A.C., 2005. Structure elucidation of hexabromocyclododecanes – a class of compounds with a complex stereochemistry. Chemosphere 61, 65–73.

Heeb, N.V., Schweizer, W.B., Mattrel, P., Haag, R., Kohler, M., 2007a. Crystal structure analysis of enantiomerically pure (+) and (-) β-hexabromocyclododecanes. Chemosphere 66, 1590–1594.

Heeb, N.V., Schweizer, W.B., Mattrel, P., Haag, R., Gerecke, A.C., Kohler, M., Schmid, P., Zennegg, M., Wolfensberger, M., 2007b. Solid-state conformations and absolute configurations of (+) and (-) α- β and γ -hexabromocyclododecanes (HBCDs). Chemosphere 68, 940–950.

Heeb, N.V., Zindel, D., Graf, H., Azara, V., Schweizer, W.B., Geueke, B., Kohler, H.-P.E., Lienemann, P., 2013. Stereochemistry of LinB-catalyzed biotransformation of δ-HBCD to 1R,2R,5S,6R,9R,10S-pentabromocyclododecanol. Chemosphere 90, 1911–1919.

Heeb, N.V., Wyss, A.S., Geueke, B., Fleischmann, T., Kohler, H.-P.E., Lienemann, P., 2014. LinA2, a HCH-converting bacterial enzyme that dehydrohalogenates HBCDs. Chemosphere 107, 194–202.

Heeb, N.V., Wyss, S.A., Geueke, B., Fleischmann, T., Kohler, H.-P.E., Schweizer, W.B., Moor, H., Lienemann, P., 2015. Stereochemistry of enzymatic transformations of (+)β- and (-)β -HBCD with LinA2 – a HCH-degrading bacterial enzyme of Sphingobium indicum B90A. Chemosphere 122, 70–78.

Heeb, N.V., Mazenauer, M., Wyss, S., Geueke, B., Kohler, H.-P.E., Lienemann, P., 2018. Kinetics and stereochemistry of LinB-catalyzed δ-HBCD transformation: comparison of in vitro and in silico results. Chemosphere 207, 118–129.

Heeb, N.V., Schalles, S., Lehner, S., Schinkel, L., Schilling, I., Lienemann, P., Bogdal, C., Kohler, H.-P.E., 2019. Biotransformation of short-chain chlorinated paraffins (SCCPs) with LinA2: a HCH and HBCD converting bacterial dehydrohalogenase. Chemosphere 226, 744–754.

Imai, R., Nagata, Y., Fukuda, M., Takagi, M., Yano, K., 1991. Molecular cloning of a Pseudomonas paucimobilis gene encoding a 17-kilodalton polypeptide that eliminates HCl molecules from γ-hexachlorocyclohexane. J. Bacteriol. 173, 6811–6819.

Janak, K., Covaci, A., Voorspoels, S., Becher, G., 2005. Hexabromocyclododecane

(HBCD) in marine species from the Western Scheldt Estuary: diastereomer- and enantiomer-specific accumulation. Environ. Sci. Technol. 39, 1987–1994.

Kohler, M., Zennegg, M., Bogdal, C., Gerecke, A.C., Schmid, P., Heeb, N.V., Sturm, M., Vonmont, H., Kohler, H.-P., Giger, W., 2008. Temporal trends, congener patterns, and sources of octa-, nona-, and decabromodiphenyl ethers (PBDE) and hexabromocyclododecanes (HBCD) in Swiss lake sediments. Environ. Sci. Technol. 42, 6378–6384.

Kumari, R., Subudhi, S., Suar, M., Dhingra, G., Rainia, V., Dogra, C., Lal, S., van der Meer, J.R., Holliger, C., Lal, R., 2002. Cloning and characterization of lin genes responsible for the degradation of hexachlorocyclohexane isomers by Sphingomonas paucimobilis strain B90. Appl. Environ. Microbiol. 68, 6021–6028.

Lal, R., Dogra, C., Malhotra, S., Sharma, P., Pal, R., 2006. Diversity, distribution and divergence of lin genes in hexachlorocyclohexane-degrading sphingomonads. Trends Biotechnol. 24, 121–130.

Lal, R., Pandey, G., Sharma, P., Kumari, K., Malhotra, S., Pandey, R., Raina, V., Kohler, H.-P.-E., Holliger, C., Jackson, C., Oakeshott, J.G., 2010. Biochemistry of microbial degradation of hexachlorocyclohexane and prospects for bioremediation. MMBR (Microbiol. Mol. Biol. Rev.) 74, 58–80.

Law, R.J., Kohler, M., Heeb, N.V., Gerecke, A.C., Schmid, P., Voorspoels, S., Covaci, A., Becher, G., Janak, K., Thomsen, C., 2005. Hexabromocyclododecanes challenge scientists and regulators. Environ. Sci. Technol. 39, 281A–287A.

Li, Y.F., 1999. Global technical hexachlorocyclohexane usage and its contamination consequences in the environment: from 1948 to 1997. Sci. Total Environ. 232, 121–158.

Marvin, C.H., Tomy, G.T., Armitage, J.M., Arnot, J.A., McCarty, L., Covaci, A., Palace, V., 2011. Hexabromocyclododecane: current understanding of chemistry, environmental fate and toxicology and implications for global management. Environ. Sci. Technol. 45, 8613–8623.

Nagasawa, S., Kikuchi, R., Nagata, Y., Takagi, M., Matsuo, M., 1993. Stereochemical analysis of γ-HCH degradation by Pseudomonas paucimobilis UT26. Chemosphere 26, 1187–1201.

Nagata, Y., Hatta, T., Imai, R., Kimbara, K., Fukuda, M., Yano, K., Takagi, M., 1993. Purification and characterization of γ-hexachlorocyclohexane (γ-HCH) dehydrochlorinase (LinA) from Pseudomonas paucimobilis. Biosci. Biotechnol. Biochem. 57, 1582–1583.

Nagata, Y., Miyauchi, K., Takagi, M., 1999. Complete analysis of genes and enzymes for γ-hexachlorocyclohexane degradation in Sphingomonas paucimobilis UT26. J. Ind. Microbiol. Biotechnol. 23, 380–390.

Nagata, Y., Endo, R., Ito, M., Ohtsubo, Y., Tsuda, M., 2007. Aerobic degradation of lindane (γ-hexachlorocyclohexane) in bacteria and its biochemical and molecular basis. Appl. Microbiol. Biotechnol. 76, 741–752.

Okai, M., Kubota, K., Fukuda, M., Nagata, Y., Nagata, K., Tanokura, M., 2010. Crystal structure of γ-hexachlorocyclohexane dehydrochlorinase LinA from Sphingobium indicum UT26. J. Mol. Biol. 403, 260–269.

Pal, R., Bala, S., Dadhwal, M., Kumar, M., Dhingra, G., Prakash, O., Prabagaran, S.R., Shivaji, S., Cullum, J., Holliger, C., Lal, R., 2005. Hexachlorocyclohexane-degrading bacterial strains Sphingomonas paucimobilis B90A, UT26 and Sp+, having similar lin genes, represent three distinct species, Sphingobium indicum sp. nov., Sphingobium japonicum sp. nov. and Sphingobium francense sp. nov., and reclassification of [Sphingomonas] chungbukensis as Sphingobium chungbukense comb. nov. Int. J. Syst. Evol. Microbiol. 55, 1965–1972.

Peck, A.M., Pugh, R.S., Moors, A., Ellisor, M.B., Porter, B.J., Becker, P.R., Kucklick, J.R., 2008. Hexabromocyclododecane in white-sided dolphins: temporal trend and stereoisomer distribution in tissues. Environ. Sci. Technol. 42, 2650–2655.

Suar, M., Hauser, A., Poiger, T., Buser, H.-R., Müller, M.D., Droga, C., Raina, V., Holliger, C., van der Meer, J.R., Lal, R., Kohler, H.-P.E., 2005. Enantioselective transformation of α-hexachlorocyclohexane by the dehydrochlorinases LinA1 and LinA2 from the soil bacterium Sphingomonas paucimobilis B90A. Appl. Environ. Microbiol. 12, 8514–8518.

Shrivastava, N., Macwan, A.S., Kohler, H.-P.E., Kumar, A., 2017. Important amino acid residues of hexachlorinases (LinA) for enantioselective transformation of hexachlorocyclohexane isomers. Biodegradation 28, 171–180.

Tomy, G.T., Budakowski, W., Halldorson, T., Whittle, D.M., Keir, M.J., Marvin, C., Macinnis, G., Alaee, M., 2004. Biomagnification of alpha- and gamma-hexabromocyclododecane isomers in a Lake Ontario food web. Environ. Sci. Technol. 38, 2298–2303.

Trantirek, L., Hynkova, K., Nagata, Y., Murzin, A., Ansorgova, A., Sklenar, V., Damborsky, J., 2001. Reaction mechanism and stereochemistry of gamma-hexachlorocyclohexane dehydrochlorinase LinA. J. Biol. Chem. 276, 7734–7740.

Trott, O., Olson, A.J., 2010. AutoDock Vina: improving the speed and accuracy of docking with a new scoring function, efficient optimization, and multithreading. J. Comput. Chem. 31, 455–461.

UNEP, 2006. United Nations Environment Programme. Report of the Conference of the Parties of the Stockholm Convention on Persistent Organic Pollutants on the Work of its Second Meeting. Risk Profile on Lindane. UNEP/POPS/POPRC. .2/17/Add.4, 21. November 2006.

UNEP, 2009. United Nations Environment Programme. Report of the Conference of the Parties of the Stockholm Convention on Persistent Organic Pollutants on the Work of its Fourth Meeting. UNEP/POPS/COP4/38 8. May 2009.

UNEP, 2013. United Nations Environment Programme. Report of the Conference of the Parties of the Stockholm Convention on Persistent Organic Pollutants on the Work of its Sixth Meeting. UNEP/POPS/COP6. June 2013.

Vijgen, J., Abhilash, P.C., Li, Y.F., Lal, R., Forter, M., Torres, J., Singh, N., Yunus, M., Tian, C., Schäffer, A., Weber, R., 2011. Hexachlorocyclohexane (HCH) as new Stockholm Convention POPs - a global perspective on the management of

Lindane and its waste isomers. Environ. Sci. Pollut. Res. Int. 182, 152−162.

Vorkamp, K., Bester, K., Riget, F.F., 2012. Species-specific time trends and enantiomer fractions of hexabromocyclododecane (HBCD) in biota from East Greenland. Environ. Sci. Technol. 46, 10549−10555.

Zegers, B.N., Mets, A., van Bommel, R., Minkenberg, C., Hamers, T., Kamstra, J.H., Pierce, G.J., Boon, J.P., 2005. Levels of hexabromocyclododecane in harbour porpoises and common dolphins from Western European seas, with evidence for stereoisomer-specific biotransformation by cytochrome P450. Environ. Sci. Technol. 39, 2095−2100.